International Journal of Heat and Mass Transfer 51 (2008) 5033–5039

Contents lists available at ScienceDirect

International Journal of Heat and Mass Transfer

journal homepage: www.elsevier.com/locate/ijhmt

Investigation on operational characteristics of a miniature automatic cooling device

Qiang Li, Wenlei Lian, Hui Sun, Yimin Xuan *

School of Power Engineering, Nanjing University of Science and Technology, Nanjing 210094, China

ARTICLE INFO

Article history:
Received 4 September 2007
Received in revised form 3 April 2008
Available online 9 June 2008

Keywords:
Automatic cooling
Temperature-sensitive magnetic fluids
Thermo-magnetic effect
Parameter estimation

ABSTRACT

The magnetocaloric effect is a well-known phenomenon, which can be applied to develop a system for the magnetic conversion of heat to work or automatic cooling of a working fluid without any mechanical pump. A prototype of a miniature automatic cooling device is established, which is mainly composed of a temperature-sensitive magnetic fluid, a permanent NdFeB magnet, heat sources and heat sink. A series of experiments are conducted to investigate the feasibility, the performance capacity of the cooling device. A model for simulating the operation process is provided and the principle of parameter estimation is applied to determine the flow velocity of the fluid in the loop. The effects of several factors such as the external magnetic field and the temperature distribution of the magnetic fluid on the cooling performance of the device are discussed.

1. Introduction

Magnetic fluid (MF) is a colloidal suspension consisting of a carrier liquid and magnetic nanoparticles with a size of about 10 nm in diameter coated with a surfactant layer. The magnetic fluid possesses not only the flowability of common Newtonian carrier fluids, but also the magnetic features being similar to those of the bulk magnetic materials. Since the magnetic fluid exhibits some unique characteristics under the influence of external magnetic fields such as magneto-viscous effect, magneto-thermal effect and magneto-optical effect, they have found many applications in mechanical engineering, bioengineering, and thermal engineering, etc. [1–4]. For most of temperature-sensitive magnetic materials, they may experience degradation in magnetization as temperature increases and lose their magnetization at the material's Curie point. Mixing of nanoparticles made from these magnetic materials into a base liquid forms a temperature-sensitive magnetic fluid.

A temperature-sensitive magnetic fluid means that its magnetization is a function of temperature. When this type of magnetic fluid experiences a temperature variation in the presence of an external magnetic field, a magnetic force will arise to drive the magnetic fluid flow, which is the fundamental principle of an automatic cooling device using temperature-sensitive magnetic fluid as a coolant. The magnitude of the driving force is a function of several factors such as the magnetic feature of the magnetic fluid, the temperature distribution, and the intensity and orientation of the external magnetic field. Since no mechanical moving part is needed in the whole device, it has great application potentials in a variety of branches of thermal engineering, especially for thermal management of spacecraft. Here one must pay attention to selecting the magnetic fluid and the ideal fluid would have a Curie point close to the maximum operating temperature of the system. There were some efforts of trying to put the magnetocaloric effect into practical application [5–9]. One of recent examples is that Love et al. [10] developed a magnetocaloric pump by exposing a 2-mm-diameter glass tube with a 40-mm-long column of a Mn–Zn ferrite magnetic fluid to a uniform magnetic field and a temperature field. They observed that the magnetic fluid moved at velocities of $1 \sim 2$ mm/s inside the tube.

In the present paper, a miniature device consisting of Mn–Zn ferrite magnetic fluid loop, a permanent magnet, a heat source, and a heat sink is established to validate the automatic cooling concept based on the thermo-magnetic principle. In such a device, the magnetic force resulting from the synergic effect of the external magnetic field and the temperature variation drives the fluid in a loop. The temperature profiles and the flow velocity of the magnetic fluid are provided for a series of operational conditions. From these data, the constitutive thermal, magnetic, and fluid dynamic relationships of the device are discussed. Through such investigations, one can get insight into the operation mechanism of the automatic cooling device, improve performance of the device, and promote the reliability of the device for different application purposes.

2. Experimental rig

It is well-known that a magnetic fluid with a large pyromagnetic coefficient $\frac{\partial M}{\partial T}$ and a low Curie point will be beneficial for establishing a high efficient automatic energy transport device. Here the temperature-sensitive Mn–Zn magnetic fluid is employed.

* Corresponding author. Tel.: +86 25 84315700; fax: +86 25 84315991.
E-mail address: ymxuan@mail.njust.edu.cn (Y. Xuan).

0017-9310/$ - see front matter © 2008 Published by Elsevier Ltd.
doi:10.1016/j.ijheatmasstransfer.2008.04.031

Nomenclature

A	cross-section area of the tube, m^2	R	tube radius, m
B	magnetic flux density along the z-direction, $N\,A^{-1}\,m^{-1}$	T	temperature, K
c_p	specific heat capacity, $J\,kg^{-1}\,K^{-1}$)	T_{hs}	temperature of the heat sink, K
$\mathbf{F}$	force per unit volume, $N\,m^{-3}$	T_{in}	temperature of fluid at the inlet of heat source, K
$\mathbf{F}_i$	force on the fluid with a finite volume, N	T_{out}	temperature of fluid at the outlet of heat source, K
$\mathbf{F}_{\sum}$	force on the whole fluid, N	$\mathbf{U}$	velocity vector, $m\,s^{-1}$
H	magnetic field intensity, $A\,m^{-1}$	u	velocity components, $m\,s^{-1}$
k	thermal conductivity, $W\,m^{-1}\,K^{-1}$	V	volume, m^3
L	length of the tube, m	v	averaged velocity along the z-direction, $m\,s^{-1}$
M	magnetization along the z-direction, $A\,m^{-1}$	v_f	kinematic viscosity, $m^2\,s^{-1}$
$\dot{m}$	mass flow rate, $kg\,s^{-1}$	μ	dynamic viscosity, $kg\,m^{-1}\,s^{-1}$
P	pressure, Pa	μ_0	permeability of free space, $N\,A^{-2}$
Q	heat load, W	ρ	density, $kg\,m^{-3}$

The working medium is a hydrocarbon based Mn–Zn ferrite magnetic fluid (BORON RUBBERS, India). Here the saturation magnetization of the sample magnetic fluid is $6.5 \times 104\,A\,m^{-1}$, the Curie temperature is 353 K and the boiling temperature is about 348–353 K. The averaged diameter for Mn–Zn ferrite magnetic particles is about 6.8 nm and the volume fraction is about 4.5%. The automatic energy transport loop is schematically shown in Fig. 1. The Mn–Zn ferrite magnetic fluid flows through a 100 mm × 80 mm loop made from 4-mm-diameter glass tube. A coil of wire of 40 mm in length is used as an electric heater by conducting direct current (DC), which is wrapped around the glass tube. The location of the heater may be changeable among three representative positions along the loop, which is labeled by heater 1, heater 2, and heater 3, respectively. A cooling chamber whose outer diameter is 30 mm and length is 60 mm is integrated with the loop. The coolant of ethylene glycol circulates through the cooling chamber, so that heat is transported from the magnetic fluid inside the loop to the coolant. The heater and heat sink may be deployed at different positions as required. A NdFeB circle magnet may be put either at r position A or symmetrically at position D which is 10 mm away from the loop and is centered along with the channel axis.

Fourteen type-K thermocouples are immersed in the loop tube to monitor the temperature profiles of the magnetic fluid. The data acquisition system is employed to read the experimental data. As shown in Fig. 1, the thermocouples TC1, TC2 and TC3 are located near the heat sink. The thermocouples TC4, TC5 and TC6 are installed along the heater 3 to monitor the inlet (outlet), middle, and outlet (inlet) temperature of the heating section. Similarly, the thermocouples TC12, TC13 and TC14 are used mainly for the case that heater 1 is in operation and the thermocouples TC9, TC10 and TC11 are for the case that the heat source is at the position of heater 2. The thermocouples from TC7 to TC11 are located along the AD section of the loop. Before they are installed, all of the thermocouples are accurately calibrated by the temperature-controlled water bath with the temperature range from 283 to 363 K.

The entire loop is thermally insulated with sponge to reduce the heat loss from the loop to the ambient. The coolant in the ethylene glycol loop is cooled by a constant low-temperature bath with a fine control uncertainty of ±0.1 K. Before the experiments, the external magnetic field H along the axial direction of the loop is carefully measured with a Gaussmeter (LAKESHORE Inc., Serial 410) for both the cases that the NdFeB magnet is respectively displaced to the position A or D. The maximum uncertainty of the Gaussmeter is 2%. The distribution of the magnetic field for the case that the magnet is displaced to position A is indicated in Fig. 2. Since the magnet location A and D are symmetrical, the measurement procedure is similar and the distributions of the

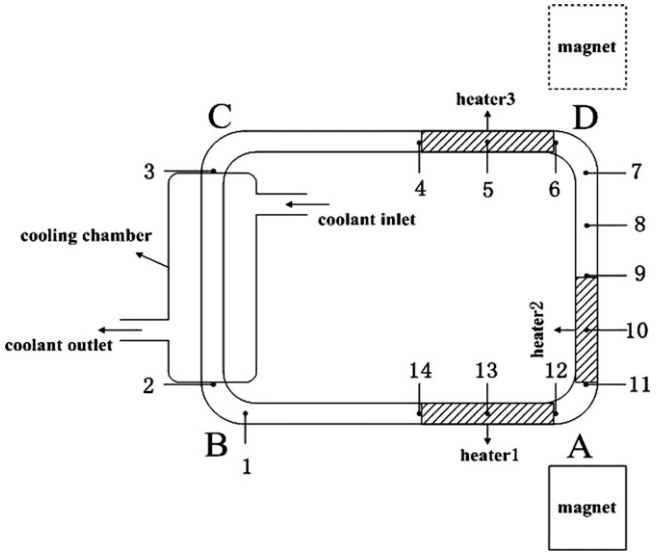

Fig. 1. Schematic diagram of a miniature automatic cooling device.

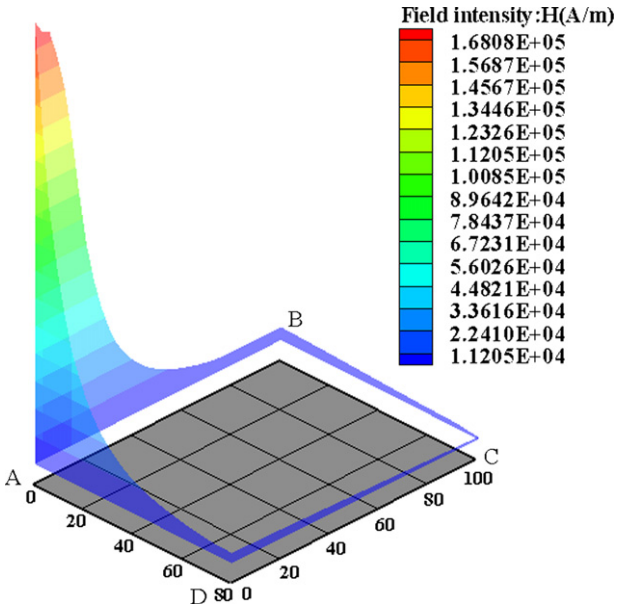

Fig. 2. Distribution of the magnetic field.

magnetic field corresponding to the magnet position D are not illustrated.

3. Models of magnetic fluid flow and temperature in a channel

As mentioned before, a temperature-sensitive magnetic fluid exhibits a field-induced flow when it is exposed to the coincident magnetic and thermal fields, which is the fundamental principle of inventing an automatic energy transport device. The coupling function of the magnetic and thermal field results in a variable Kelvin force acting on the fluid and finally produces a magnetic pressure to drive the fluid. Consider coordinate z along the central axis of the loop. On the assumption of the incompressible fluid, the Navier–Stokes equation applies to the flow inside the loop as follows:

$$\frac{\partial P}{\partial z} = \mu \frac{1}{r} \frac{\partial}{\partial r}\left(r \frac{\partial u_z}{\partial r}\right) \tag{1}$$

where u_z represents the velocity component which is along z direction and $\partial P/\partial z$ is the total pressure gradient.

By considering the no-slip boundary ($r = R$) and the finite velocity at the center of the pipe ($r = 0$), the velocity distribution of the magnetic fluid in the channel is

$$u_z(r) = -\frac{R^2}{4\mu} \frac{\partial P}{\partial z}\left(1 - \left(\frac{r}{R}\right)^2\right) \tag{2}$$

The averaged velocity v can be expressed as the ratio of the fluid flow over the cross-sectional area of the channel:

$$v = \frac{\int_0^R u_z(r) 2\pi r \, dr}{\pi R^2} = -\frac{R^2}{8 v_f} \frac{\partial P}{\partial z} \tag{3}$$

Love et al. derived the force density experienced by the magnetic fluid [10]:

$$\mathbf{F} = \mathbf{B}(\nabla \cdot \mathbf{H}) + \frac{1}{2}\mu_0 \left(\mathbf{H} \cdot \frac{\partial \mathbf{M}}{\partial T}\right) \nabla T \tag{4a}$$

For the present experimental system, its scalar form is as follows:

$$F = B \frac{\partial H}{\partial z} + \frac{1}{2}\mu_0 H \frac{\partial M}{\partial T} \frac{\partial T}{\partial z} \tag{4b}$$

The first term in expression (4a) or (4b) is the magnetic pressure induced by the non-uniform magnetic field [11] and the second term is the magnetocaloric force resulting from the magnetocaloric effect of the magnetic fluid. For the temperature-sensitive magnetic fluid, the pyromagnetic coefficient $\frac{\partial M}{\partial T}$ is not equal to zero near the Curie temperature point and so that the second term in expression (4) is generally not negligible. Thus, the force density acting on the magnetic fluid is dependent not only upon the magnitude of the magnetic field intensity and but also upon the temperature gradient of the magnetic fluid whose magnetization is a temperature-sensitive function. In addition, it is related with the synergy of the orientations of both the external magnetic field and the temperature gradient. By altering either the magnitudes and/or the directions of these force vectors, one may adjust the force density for the purpose of controlling the flow and heat transfer processes in the magnetic fluid loop.

For volume ΔV of the magnetic fluid, such a force is expressed as

$$F_i = \left(B \frac{\partial H}{\partial z} + \frac{1}{2}\mu_0 H \frac{\partial M}{\partial T} \frac{\partial T}{\partial z}\right) \Delta V \tag{5}$$

By considering the whole fluid as an ensemble of n fixed volume of fluid (dV), the force acting on this whole fluid system is expressed as

$$F_{\sum} = \sum_{i=1}^{n} F_i \tag{6}$$

According to Eqs. (3), (5) and (6), one may have

$$-\frac{\partial P}{\partial z} = \frac{\sum_{i=1}^{n} F_i}{AL} = \frac{\sum_{i=1}^{n} F_i}{\pi R^2 L} \tag{7}$$

$$v = \frac{F_{\sum}}{8\mu\pi L} \tag{8}$$

Here it is obvious that one must get the magnetic driving force large enough to overcome the flow resistance along the flow channel to maintain a stable and continuous flow.

The energy equation of the magnetic fluid can be expressed as follows [12]:

$$\rho c_p \frac{DT}{Dt} + \mu_0 T \left(\frac{\partial \mathbf{M}}{\partial T}\right)_{V,H} \cdot \frac{D\mathbf{H}}{Dt} = k\nabla^2 T \tag{9}$$

From these equations, one can numerically simulate the flow and temperature distributions of the magnetic fluid under the given external magnetic field and non-uniform thermal conditions.

4. Results and discussions

Since the temperature gradient inside the magnetic fluid will affect the magnetic driving force according to Eq. (4), one can control the temperature distribution of the fluid by changing the position and the heat load of the heater. In such approaches, one may maintain the optimal synergy of the temperature gradient and the external magnetic field in order to bring as large magnetic driving force as possible.

When the magnet is displaced to the position A (as shown in Fig. 2), section CB and section DC of the loop are far away from the external magnet and the magnetic fluid in these two sections may experience a small magnetic field gradient, so that the forces $\mathbf{F}_{CB}$ and $\mathbf{F}_{DC}$ being acted on these two sections are quite small compared with those $\mathbf{F}_{AD}$ and $\mathbf{F}_{BA}$ on the other two sections AD and BA. Both the forces $\mathbf{F}_{AD}$ and $\mathbf{F}_{AB}$ were pointed to A along the axis of the tube. If the magnitudes of these two forces were equal to each other, the magnetic fluid could not move in the loop.

Being prior to applying heat load to the loop through heater 2, the coolant of ethylene glycol flowed through the heat sink and its temperature was kept at 271 K. Fig. 3a shows a steady-sate temperature profile of the magnetic fluid in the cases that the input heat load was 3.5 W from heater 2 and the magnet is displaced to the position A. The results reveal that the magnetic fluid flow experiences a start-up process in which the fluid temperature changes with the time. The flow and temperature of the fluid approach steady-state distribution after a short time span. Smaller fluctuation in the fluid temperature may result from the fluctuation in the volume fraction of the magnetic nanoparticles during the fluid flow in the channel. An interesting phenomenon is observed that the readings of thermocouple TC9 and TC11 are not identical although they are symmetrically deployed at the opposite ends of heater 2. In fact, the steady-state temperature of TC9 is 56.4 K higher than that of TC11, which just indicates the steady circulation flow of the magnetic fluid in the loop was formed under the effects of the resulting magnetic driving force. Otherwise, both the readings from these two thermocouples should be the same if heat conduction were the energy transport mode inside the magnetic fluid. In fact, the magnetic fluid flowed anticlockwise. Therefore, the convective equation rather than heat conduction equation should be used to describe the temperature profile of the magnetic fluid. The relatively lower temperature readings from thermocouples TC12, TC13 and TC14 in section BA of the loop further validate such a phenomenon.

For the purpose of comparison, another run of experiment was conducted under the same conditions as those above-mentioned except that the external magnetic field was absent. The tempera-

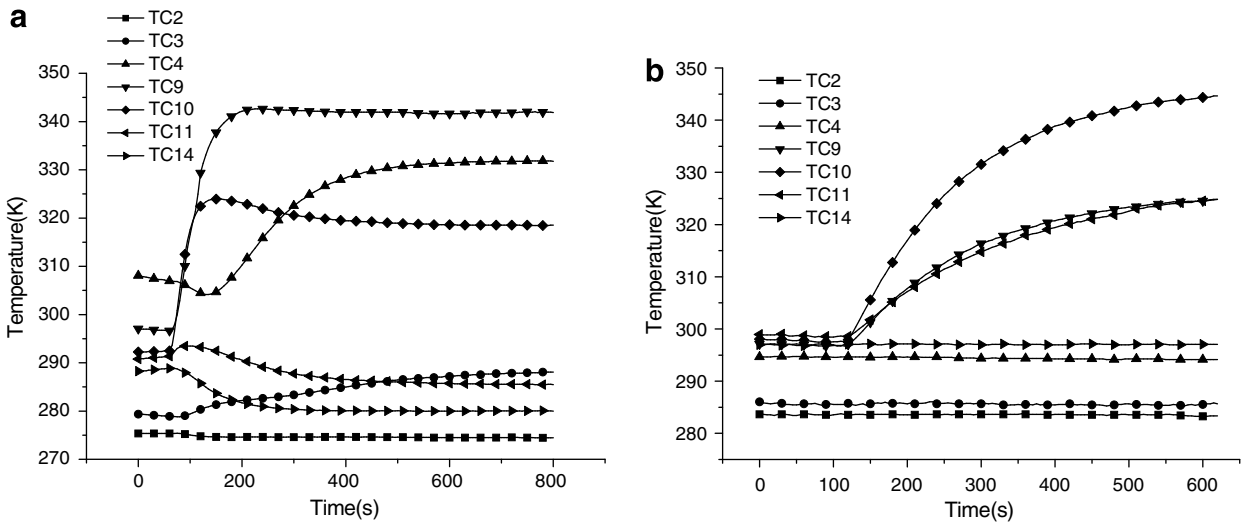

Fig. 3. Temperature profiles of the magnetic fluid: (a) in the presence of a magnet and (b) in the absence of a magnet.

ture profile of the magnetic fluid is shown in Fig. 3b. Obviously, the readings from the thermocouples of TC9 and TC11 are symmetrically almost the same, which indicates that heat conduction is the main mode of energy transport inside the fluid and no macroscopic convection takes place in the loop. Such experimental data further confirm that the observed temperatures shown in Fig. 3a

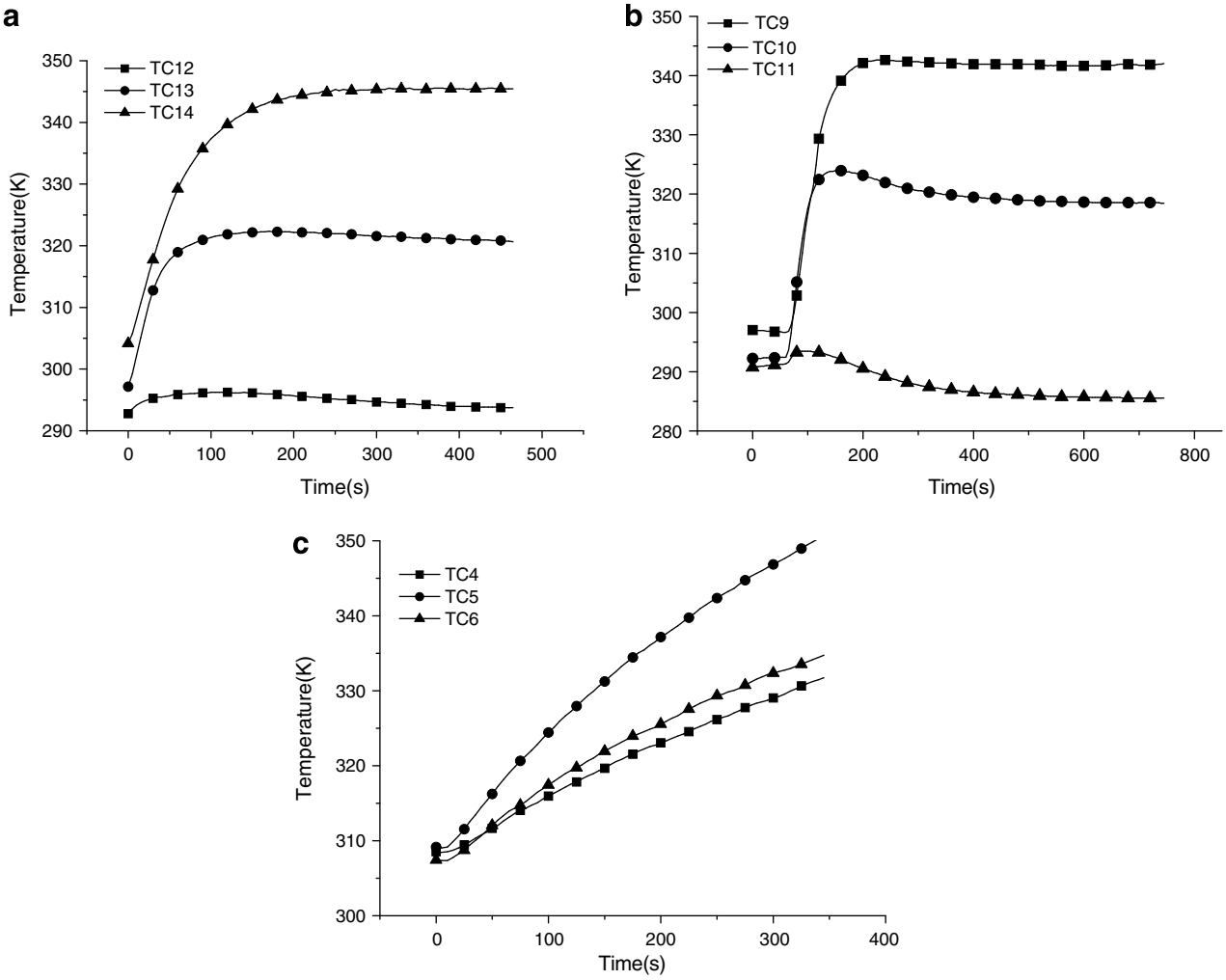

Fig. 4. The effect of heat sources: (a) heater 1, $Q = 2.91$ W; (b) heater 2, $Q = 3.53$ W and (c) heater 3, $Q = 1.02$ W.

result from the flow phenomenon because of the synergic function between the external magnetic field and the thermal field. It is so-called the field-induced pumping flow.

For the steady state of experiment runs, the principle of energy balance is applied to estimate the average velocity of the working fluid from the heat power and the temperature distribution of the fluid in the channel. By neglecting the heat loss from the loop to the ambient, we considered all of was transferred to the passing fluid. The relationship between the energy input Q from the electric heater (i.e., the heat load of the cooling loop) and the average velocity of the fluid is expressed as follow:

$$Q = \dot{m}c_p(T_{\text{out}} - T_{\text{in}}) = \rho c_v v A(T_{\text{out}} - T_{\text{in}}) \tag{10}$$

From this formula, the flow velocity corresponding to the experimental data of Fig. 3a is estimated to be 2.1 mm/s.

More generally, the unknown flow velocity of the magnetic fluid in the loop can be determined with the parameter estimation method [13]. The velocity of the magnetic fluid can be determined from the following least square error relationship between the estimated temperatures $T(z_i, t_j)$ and experimental readings $T_{\text{exp}}(z_i, t_j)$:

$$\min S(z,t) = \sum_i \sum_j \|T(z_i,t_j) - T_{\text{exp}}(z_i,t_j)\|^2 \tag{11}$$

The estimated temperatures $T(z_i,t_j)$ are obtained from the solution of the above-mentioned equations as a direct problem.

Since there exist the non-uniform temperature and magnetic fields inside the whole loop, the net magnetic driving force arises and the fluid circulates in the loop. By altering the load and/or position during the experiment, one can easily adjust the flow and temperature distribution of the magnetic fluid along the whole loop. Fig. 4 indicates the effects of the position and heat flux of the electric heater to find a suitable position of the heat source in the loop. From the temperature profiles shown in Fig. 4a, one can learn that a heater at the position of heater 1 was put into operation, the magnetic fluid performed a clockwise flow. The input heat load was 2.91 W and the peak value of temperature of the fluid (just at the outlet of the heating section) was 345.4 K. The estimated averaged velocity of the fluid in the loop was v = 1.91 mm/s. When the heater moved to the position of heater 2, the peak temperature of the magnetic fluid was 341.8 K in the case of heat load 3.53 W (as shown in Fig. 4b) and the estimated velocity of the fluid was v = 2.13 mm/s. Evidently, the cooling capability of the whole loop in such a case is better than the case that former. Another example further demonstrates the importance of synergic or matching relationship between the external magnetic field and the temperature gradient (as shown in Fig. 4c)for maintaining a steady flow in the loop. When the electric heater

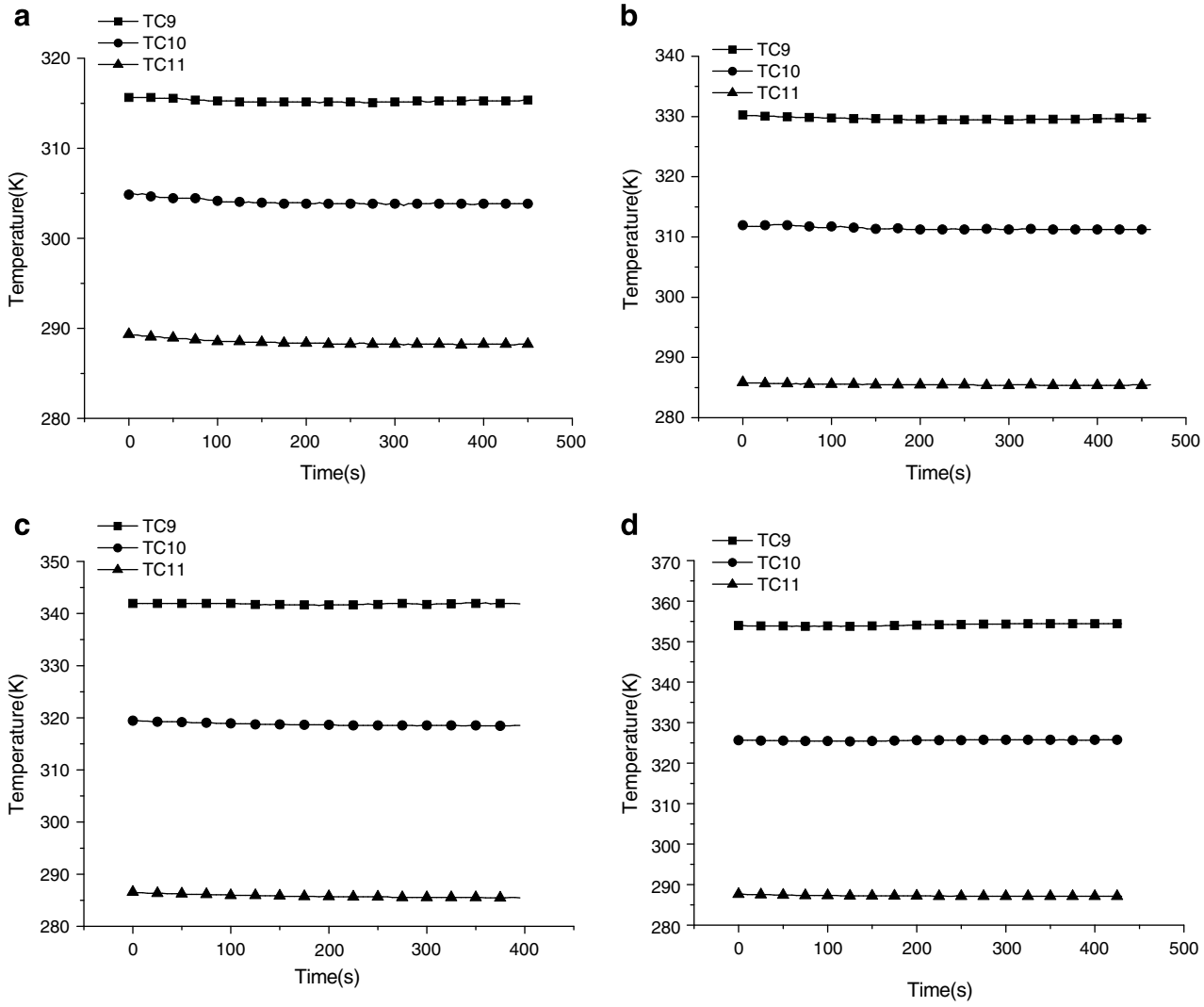

Fig. 5. Steady-state temperature of the magnetic fluid at the inlet, middle and outlet of the heating position subject to different heat loads: (a) Q = 0.92 W; (b) Q = 2.08 W; (c) Q = 3.53 W and (d) Q = 3.70 W.

was located at the position of heater 3, there was no evidence that the magnetic fluid was in flow and the estimated velocity of the fluid was approximately equal to zero. In fact, the fluid temperature readings near the two ends of the electric heater increases sharply and incessantly in such a case even the heat load was smaller, which indicated that heat conduction was the sole mode of energy transport inside the magnetic fluid and the fluid was stationary. The reason is that application of heater 3 exerted almost no influence on the forces $\mathbf{F}_{AD}$ and $\mathbf{F}_{AB}$, so little magnetic driving force was formed and the fluid failed to flow. Among the above-mentioned examples, application of heater 2 optimizes the cooling performance of the cooling device.

By keeping other conditions unchangeable, a series of experiments were conducted to examine the performance of the cooling device subjected to different heat loads from heater 2. The steady-state temperature profiles of the magnetic fluid around the heat source position are shown in Fig. 5. The peak temperature (i.e., the fluid temperature at the outlet of the heating section) is 315.3 K and 341.8 K corresponding to the heat load of 0.92 W and 3.53 W, respectively. If the heat load further increased, the peak temperature of the fluid might rise over the boiling point of the base liquid and the performance of the device would rapidly deteriorate, which should be avoided. Below such a temperature threshold, the flow velocity of the magnetic fluid increases with the heat load (as shown in Fig. 6). The reason is that a higher heat load will lead to a larger temperature gradient, and then a bigger driving force will be generated and make the magnetic fluid flow more quickly in the loop. For the heat load $Q = 3.52$ W, the estimated velocity v reached up to 2.13 mm/s. This phenomenon indicates that such a cooling device has self-regulating function: As the heat load increases, the flow velocity of the fluid increases and the heat will be more quickly transported from the heating section to the cooling section. However, the cooling capacity of the device is limited below the boiling point of the magnetic fluid. As shown in Fig. 6, it is noticeable that the average velocity abruptly fall to 1.87 mm/s when $Q = 3.70$ W instead of keeping increase tendency. This may attribute to the fact that some fluid boiled away and the generated bubbles partially blocked the channel.

In order to investigate the effect of the magnet location on the performance of the miniature automatic cooling device, the experimental runs were conducted in the case that the magnet was deployed at location D. Fig. 7 reveals a steady-sate temperature profile of the magnetic fluid for such case with the input heat load 3.53 W from heater 2 and the heat sink temperature of 271 K. Compared with the experimental data in the cases oft the magnet position A, on the contrary, it can be seen that the steady-state temperature of TC11 is higher than that of TC9. Obviously, the

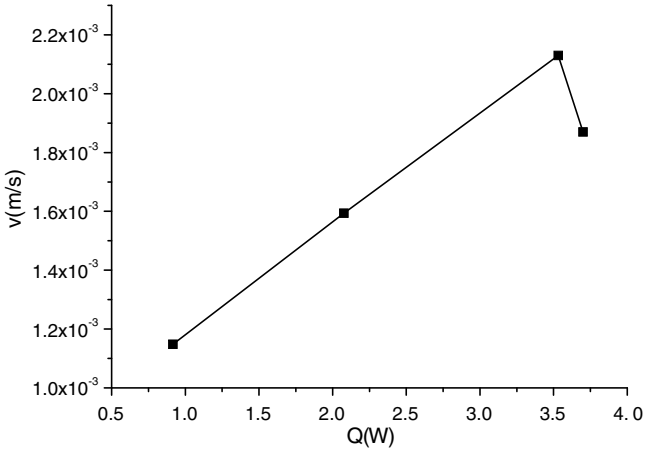

Fig. 6. Average velocity of the fluid vs the heat load.

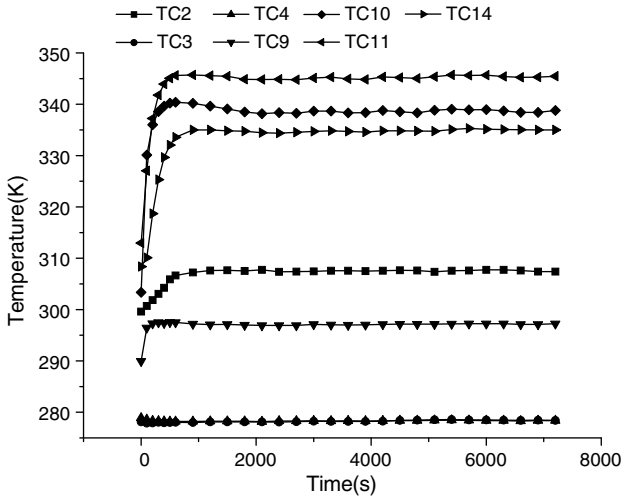

Fig. 7. Temperature profiles of the magnetic fluid in the presence of a magnet at location D.

magnetic fluid flowed clockwise in the loop, which was opposite to the flow direction corresponding to the magnet position A. The reason is that the force $\mathbf{F}_{DC}$ is remarkably augmented and becomes the primary driving force. The net magnetic driving force with the clockwise direction arises. The results have indicated that controlling flow process of magnetic fluid can be actualized by altering the location of an external magnet.

By using the above-mentioned theoretic models, one can simulate the magnetic fluid flow and temperature distribution in the loop. An example is to simulate the experimental results shown in Fig. 7. During the simulation, all the input conditions such as the loop size, the sample magnetic fluid, the input heat load, the heat sink temperature, and the magnetic field, are kept the same as the experimental conditions. The properties of the magnetic fluid involved in the simulation are listed in Table 1. Fig. 8

Table 1
Properties of the magnetic fluid in the simulation

Saturation magnetization (A m^{-1})	65 000 (measuring)
Curie point (K)	353 (measuring)
Density (kg m^{-3})	1170 (measuring)
Thermal conductivity (W m^{-1} K^{-1})	0.17 (calculated) [14]
Viscosity (m^2 s^{-1})	0.000321 (calculated) [14]
Specific heat capacity (J kg^{-1} K^{-1})	3327 (calculated) [14]
Thermo-magnetic coefficient (A m^{-1} K^{-1})	118 [15]

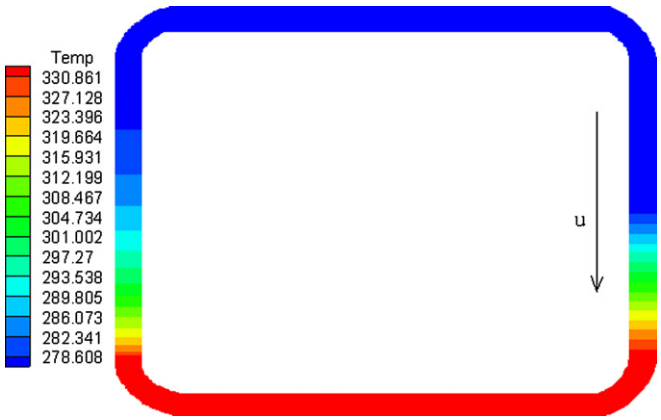

Fig. 8. Simulated temperature distribution of the magnetic fluid in the presence of a magnet at location D.

Table 2
Comparison between the theoretical and experimental results of the magnetic fluid temperature

Measuring points No.	Experimental reading (K)	Calculated result (K)	Discrepancy (K)	Error (%)
1	325.41	332.04	6.63	2.03743
2	307.18	314.56	7.38	2.4025
3	278.24	280.98	2.74	0.984761
4	278.21	280.98	2.77	0.995651
5	280.75	280.98	0.23	0.081923
7	282.68	280.98	1.7	0.601387
8	284.36	280.98	3.38	1.188634
9	297.04	294.06	2.98	1.003232
10	338.61	332.17	6.44	1.901893
11	345.26	339.67	5.59	1.61907
12	347.21	339.67	7.54	2.171596
13	340.28	339.67	0.61	0.179264
14	334.81	339.67	4.86	1.45157

illustrates the temperature distribution of the magnetic fluid in the loop and Table 2 lists the calculated steady-sate temperature at the measuring points deployed along the loop. It can be seen that the steady circulation flow of the magnetic fluid in the loop was formed and the flow direction of the magnetic fluid is along with the clockwise direction as shown in Fig. 1. Comparison between calculated results and the experimental results shows the good coincidence between both of them. The possible discrepancy between them falls below 2.5%, which reveals that the theoretic models can be used to simulate the cooling performance of the miniature automatic cooling device based on the thermo-magneto effect.

5. Conclusions

An ordered assembly of loop device consisting of the permanent NdFeB magnet, a heater, a heat sink, and a temperature-sensitive magnetic fluid can form a robust automatic cooling device. The device is maintenance-free because of no moving parts in the loop. The experiment has shown that a stable and continuous flow of the magnetic fluid can be maintained in the miniature loop and it can be used as an automatic cooling device. One of key factors for developing the device is to select a temperature-sensitive magnetic fluid with a suitable Curie point as the required coolant. The boiling-point temperature of the base liquid consisting of the magnetic fluid will affect the operating temperature range and even the cooling capacity of the device.

Since the driving force for pushing flow of the magnetic fluid results from the effect synergic of the external magnetic field and the temperature gradient, one can control the performance of the automatic cooling device by adjusting either the external magnetic field or the heater. Under the normal operating conditions, the device possesses self-adjusting function that the flow velocity of the magnetic fluid (i.e., the energy transport ability) increases with the increase in the external heat load, and vice versa, which indicates that operation of the cooling device is automatically controlled by the heat load. By altering the magnet position, one can change the flow direction of the magnetic fluid inside the loop.

The numerical algorithm has been developed and applied to simulate the performance of the miniature automatic cooling device. Comparison between the theoretical predictions and experimental data has indicated that the algorithm can provide satisfactory simulation results. The principle of parameter estimation has been applied to estimating the flow velocity of the magnetic fluid.

The following suggestions may be beneficial for developing the automatic cooling device by using a magnetic fluid as the coolant:

- To select a suitable magnetic fluid with a larger pyromagnetic coefficient, a lower Curie point, a higher saturation magnetization, a lower viscosity, and a higher boiling point.
- To exert a stronger intensity of the external magnetic field and/or a field gradient, if it is possible.
- To maintain synergy between the magnetic field and temperature gradient field.

Acknowledgement

This work is sponsored by the National Natural Science Foundation of China (Grant No. 50436020).

References

[1] K. Raj, B. Moskowitz, R. Casciari, Advances in ferrofluid technology, J. Magnet. Magnetic Mater. 149 (1995) 174–180.
[2] C. Tangthieng, B.A. Finlayson, J. Maulbetsch, T. Cader, Heat transfer enhancement in ferrofluids subjected to steady magnetic fields, J. Magnet. Magnetic Mater. 201 (1999) 252–255.
[3] A. Nethe, T. Schoppe, H. Stahlmann, Ferrofluid driven actuator for a left ventrical assist device, J. Magnet. Magnetic Mater. 201 (1999) 423–426.
[4] J.H. Liu, J.M. Gu, Z.W. Lian, H. Liu, Experiments and mechanism analysis of pool boiling heat transfer enhancement with water-based magnetic fluid, Heat Mass Transfer 41 (2004) 170–175.
[5] B. Jeyadevan, C.N. Chinnasamy, K. Shinoda, K. Tohji, H. Oka, Mn–Zn ferrite with higher magnetization for temperature sensitive magnetic fluid, J. Appl. Phys. 93 (2003) 8450–8452.
[6] T. Upadhyay, R.V. Upadhyay, R.V. Mehta, V.K. Aswal, P.S. Goyal, Characterization of a temperature-sensitive magnetic fluid, Phys. Rev. B 55 (1997) 5585–5588.
[7] K. Hishida, M. Maeda, Enhancement and control of local heat transfer coefficients in a gas flow containing soft magnetic particles, Exp. Heat Transfer 7 (1994) 55–69.
[8] K. Nakatsuka, Y. Hama, J. Takahashi, Heat transfer in temperature-sensitive magnetic fluid, J. Magnet. Magnetic Mater. 85 (1990) 207–209.
[9] H. Matsuki, K. Yamasawa, K. Murakami, Experimental considerations on a new automatic cooling device using temperature-sensitive magnetic fluid, IEEE Trans. Magnetics 13 (1977) 1143–1145.
[10] L.J. Love, J.F. Jansen, T.E. Mcknight, Y. Roh, T.J. Phelps, A magnetocaloric pump for microfluidic applications, IEEE Trans. Nanobiosci. 3 (2004) 101–110.
[11] R.E. Rosensweig, Ferrohydrodynamics, Cambridge University Press, Cambridge, 1985.
[12] H. Yamaguchi, Z.G. Zhang, S. Shuchi, K. Shimada, Gravity simulation of natural convection in magnetic fluid, JSME Int. J. Ser. B 45 (2002) 61–65.
[13] J.V. Beck, K.J. Arnold, Parameter Estimation in Engineering and Science, Wiley, New York, 1977.
[14] Decai Li, Theory and Application of Magnetic Fluids, China Science Press, 2003 (in Chinese).
[15] R. Arulmurugan, G. Vaidyanathan, S. Sendhilnathan, B. Jeyadevan, Mn–Zn ferrite nanoparticles for ferrofluid preparation Study on thermal-magnetic properties, J. Magnet. Magnetic Mater. 298 (2006) 83–94.